Neural-network-based prediction techniques for single station modeling and regional mapping of the foF2 and M(3000)F2 ionospheric characteristics

T. D. Xenos

Nonlinear Processes in Geophysics (2002) 9: 477–486

Nonlinear Processes in Geophysics

Neural-network-based prediction techniques for single station modeling and regional mapping of the *fo*F2 and M(3000)F2 ionospheric characteristics

T. D. Xenos

Aristotelian University of Thessaloniki, Dept of Electrical and Computers Eng., 54006 Thessaloniki, Greece

Received: 20 February 2002 – Revised: 19 June 2002 – Accepted: 26 June 2002

Abstract. In this work, Neural-Network-based single-station hourly daily *fo*F2 and M(3000)F2 modelling of 15 European ionospheric stations is investigated. The data used are neural networks and hourly daily values from the period 1964–1988 for training the neural networks and from the period 1989–1994 for checking the prediction accuracy. Two types of models are presented for the F2-layer critical frequency prediction and two for the propagation factor M(3000)F2. The first *fo*F2 model employs the E-layer local noon calculated daily critical frequency (foE_{12}) and the local noon F2-layer critical frequency of the previous day. The second *fo*F2 model, which introduces a new regional mapping technique, employs the Juliusruh neural network model and uses the E-layer local noon calculated daily critical frequency (foE_{12}), and the previous day F2-layer critical frequency measured at Juliusruh at noon. The first M(3000)F2 model employs the E-layer local noon calculated daily critical frequency (foE_{12}), its ± 3 h deviations and the local noon cosine of the solar zenith angle ($\cos \chi_{12}$). The second model, which introduces a new M(3000)F2 mapping technique, employs Juliusruh neural network model and uses the E-layer local noon calculated daily critical frequency (foE_{12}), and the previous day F2-layer critical frequency measured at Juliusruh at noon.

1 Introduction

The electron density height distributions of a single location find many applications both in scientific investigation and in radio-system performance assessments over neighboring paths. Moreover prediction of certain parameters, as for instance *fo*F2 and M(3000)F2 is essential for planning HF propagation radio-links. These data may be given either from measurements or by theoretical calculations. In ionospheric prediction, single-station ionospheric models posses several advantages over the rest of the methods; their cost is very low, usually they are very simple to use and in the vicinity of the station they are considerably accurate. Therefore, a number of empirical single station models (SSM) have been produced for different stations and ionospheric parameters. The activity in this area has increased as a consequence of the COST-238 and COST-251 projects. Most of the models are based on Fourier analysis (Alberca et al., 1999) or on polynomial fitting of different degree (Alberca et al., 1999; Kouris and Nissopoulos, 1994; Xenos, 1999). Several modelers introduce a second index or parameter, in addition to the solar or ionospheric index. Pancheva and Mukhtarov (1996) for instance use a parameter to determine the phase of the solar cycle that corresponds to the solar activity considered and Sole (1998) uses the magnetic index A_p together with the ionospheric index T. In most cases, *fo*F2 is the modeled ionospheric characteristic, although other parameters – mainly foE and M(3000)F2 – have been modeled too.

Neural networks have been tried in single station modelling. Williscroft and Poole (1996) have attempted to predict *fo*F2 using as training parameters the number of the day and the corresponding solar activity index, and the magnetic activity index for the period 1973–1993; the years 1989 (year of low solar activity) and 1995 (year of high solar activity) were excepted from the training and they were used for validation of the prediction. The average prediction deviation was of the order of 1.03 and 0.92 MHz respectively. Several attempts have been recently made to employ neural networks to one-hour ahead *fo*F2 prediction (Altynay et al., 1997; Cander et al., 1998). Neural Networks have been also been used in successfully temporal and spatial forecasting *fo*F2 models for four European stations with very rich past data sets (Kumulca eta al., 1997).

In the present work Neural Network based single-station hourly daily *fo*F2 and M(3000)F2 modeling of 10 European ionospheric stations is investigated. Two types of models are tested or the F2-layer critical frequency and two for the propagation factor M(3000)F2. The first *fo*F2 model employs the E-layer local-noon calculated daily critical frequency (foE_{12}) and the local noon F2-layer critical frequency of the previ-

Correspondence to: T. D. Xenos
(tdxenos@vergina.eng.auth.gr)

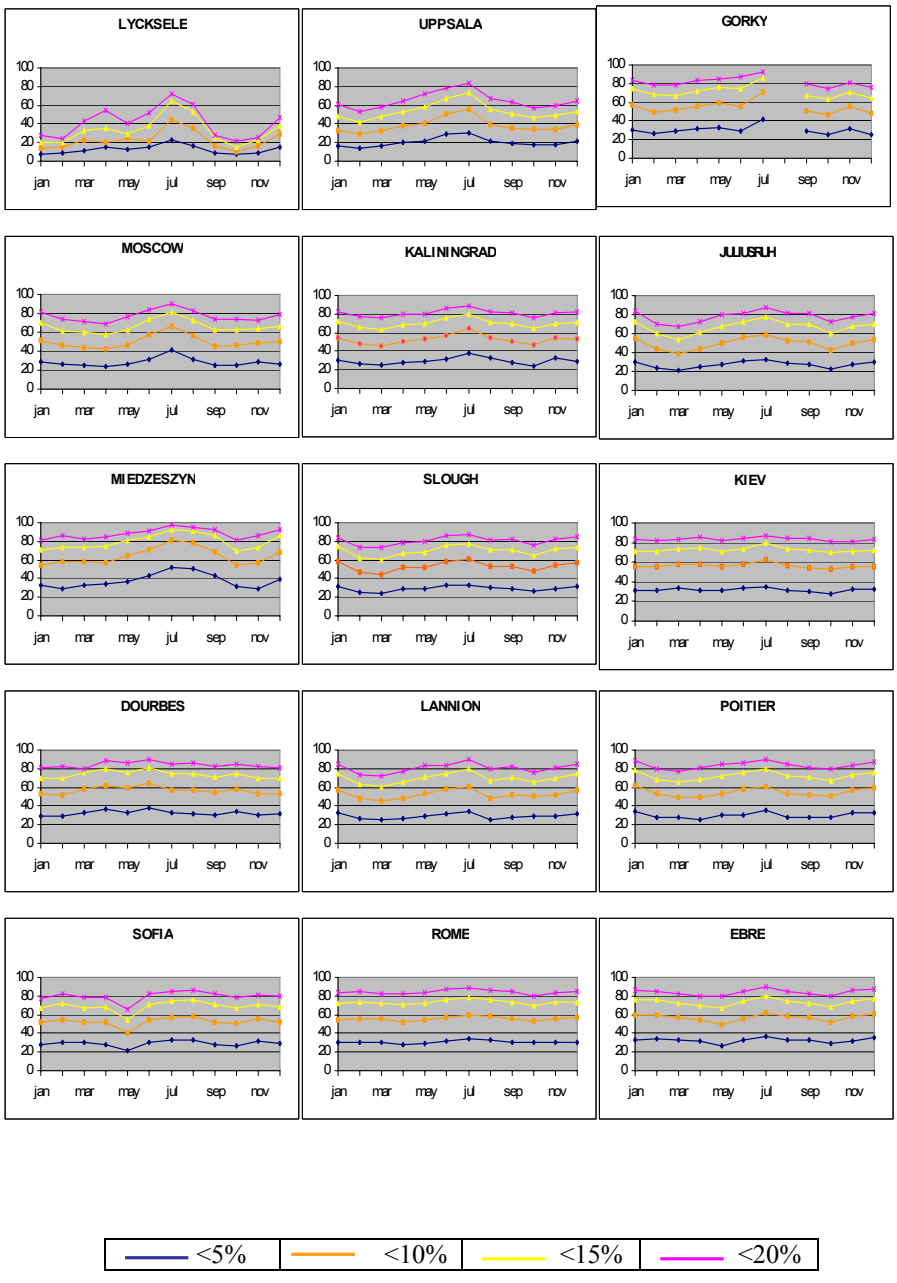

Fig. 1. Performance of the foF2 single station model for each ionospheric station.

ous day. The second *fo*F2 model, which in fact introduces a new regional mapping technique, employs the Juliusruh neural network model and uses the E-layer local noon calculated daily critical frequency (foE_{12}), and the previous day F2-layer critical frequency measured at Juliusruh at noon. The first M(3000)F2 model employs the E-layer local noon calculated daily critical frequency (foE_{12}), its ± 3 h deviations and the local noon cosine of the solar zenith angle ($\cos \chi_{12}$). The second model, which also introduces a new M(3000)F2 mapping technique, employs the Juliusruh neural network model and uses the E-layer local noon calculated daily critical frequency (foE_{12}), and the previous day F2-layer critical frequency measured at Juliusruh at noon. The predicted values are compared to the corresponding measured data and the relative errors are calculated. In this stage, the predicted periods were categorised according to the geomagnetic (with respect to A_p) and solar (with respect to R) conditions into two categories for the former, defining quiet and disturbed ionosphere, and three for the latter, describing low, medium and high solar activity. Depending on the type of data and on the month, the resulting correlation seems to vary from good to very good and what is more important, the results

Table 1. Ionospheric stations used for modelling

Station	Coordinates
Dourbes	50.1 N, 4.6 E
Ebre	40.8 N, 0.5 E
Gorky	56.1 N, 44.3 E
Juliusruh	54.6 N, 13.4 E
Kaliningrad	54.7 N, 20.6 E
Kiev	50.5 N, 30.5 E
Lannion	48.8 N, 356.6 E
Lycksele	64.7 N, 18.8 E
Miedzeszyn	52.2 N, 21.2 E
Moskow	55.5 N, 37.3 E
Poitier	46.6 N, 0.3 E
Rome	41.9 N, 12.5 E
Slough	51.5 N, 359.4 E
Sofia	42.7 N, 23.4 E
Uppsala	59.8 N, 17.6 E

do not seem to be affected considerably by geomagnetic or solar conditions. Moreover, it is worth mentioning that the new mapping technique gives very promising results compared to other existing regional mapping techniques applied in the same area.

2 Methods

The data used in the models are hourly daily values of the F2-layer critical frequency (*fo*F2) or of the propagation factor M(3000)F2, depending on the availability, for the period 1964–1988 for training the neural networks and for the period 1989–1994 for checking the data prediction accuracy. The ionospheric stations and their positions are presented in Table 1. The characteristics of the neural networks employed are presented in Table 2b whereas in Table 2a the characteristics of the Neural Networks employed for the Juliusruh models are given. All models employ the hourly-daily E-layer critical frequency calculated at noon (foE_{12}) (1) (Kouris, 1981)

$$foE^4 = (\cos\chi)^{1.2}(1 + 0.0091\,R)\,(88 + 31\cos\phi)(d^{-2})(\cos\chi_{12})^{(0.11-0.49\cos\phi)} \quad (1)$$

where:

Table 2a. Juliusruh Neural network characteristics

	*fo*F2 Model		M(3000)F2 Model	
	No. of Neurons in hidden layers			
Month	Layer 1	Layer 2	Layer 1	Layer 2
January	8	8	6	6
February	10	10	8	8
March	6	6	6	6
April	6	6	6	6
May	12	12	12	12
June	8	8	6	6
July	6	6	12	12
August	6	6	6	6
September	8	8	8	8
October	6	6	6	6
November	10	10	10	10
December	8	8	8	8

Table 2b. Neural network characteristics

Neural Network type	Multilayer perceptron
Training method	Back-Propagation, Batching
Method Optimization	Adaptive learning rate parameter and momentum constant
Neural Network structure	One input, two hidden, one output
Activation functions	tanh(x) for the hidden layers, linear for the output
Training end criterion	Cross-validation method

foE	is the E-layer critical frequency
R	is the solar sunspot index
$\cos\chi$	is the solar zenith angle cosine
$\cos\chi_{12}$	is the solar zenith angle cosine at noon
d	is the ratio of the Sun-Earth distance on the fifteenth day of each month to the average value of the year
$\cos\phi$	is the geographical latitude cosine

The characteristics of each model are presented in Table 3. The average therein deviations from the local noon foE are calculated as:

$$f'oE = (foE_{12} - foE_{av})/foE_{av} \quad (2)$$

where:

$$foE_{av} = \frac{\left[\sum_{i=9}^{11} foE_i + \sum_{i=13}^{15} foE_i\right]}{6} \quad (3)$$

3 Results

For each month and for the period 1989–1994 the observed and the corresponding estimated *fo*F2 and M(3000)F2 hourly

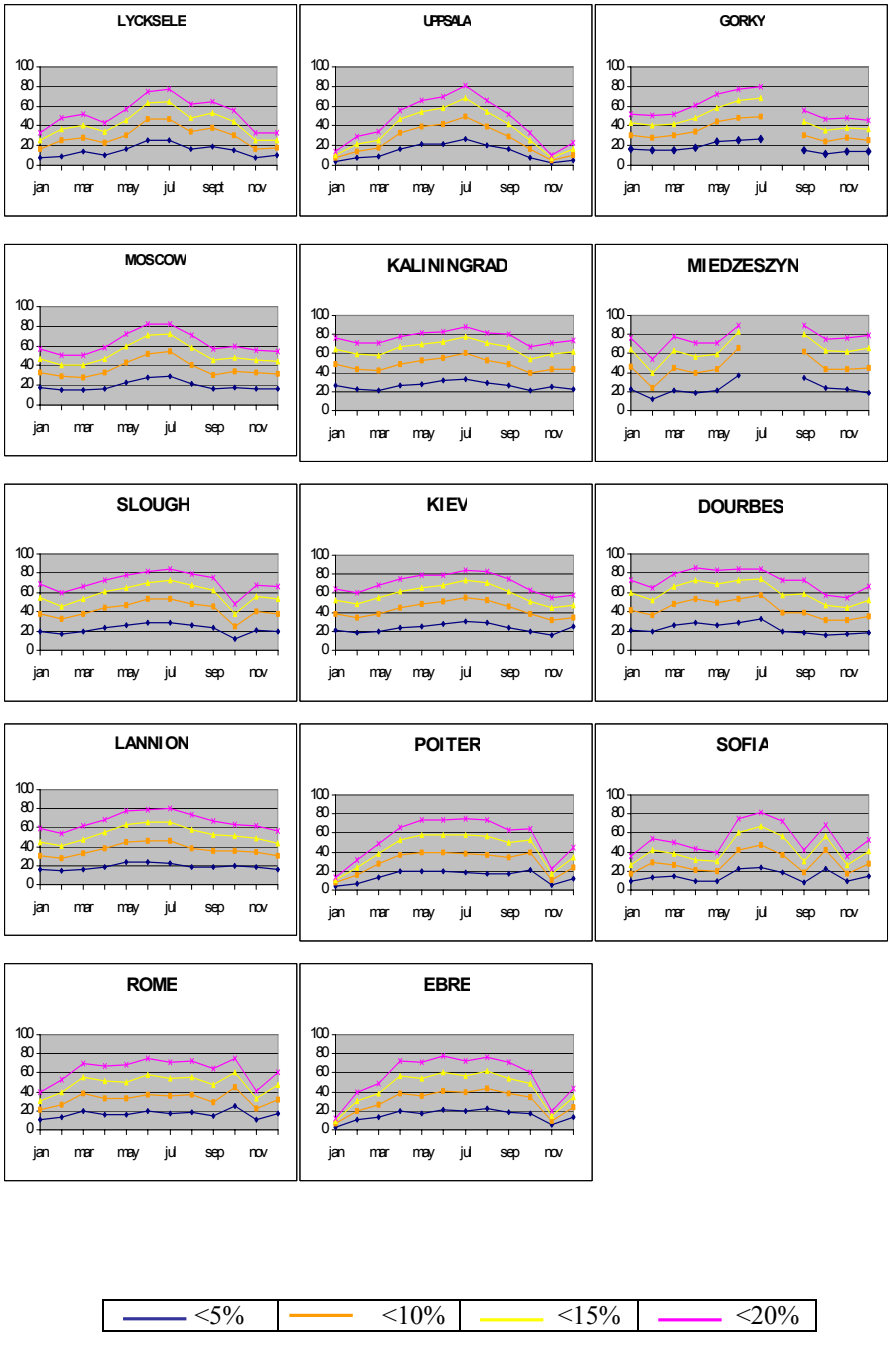

Fig. 2. Performance of the foF2 mapping at each ionospheric station.

daily values were compared and the relative error was calculated and distributed according to the achieved error to four categories, namely those of less than: 5%, 10%, 15% and 20%.

The results for the *fo*F2 models are shown in Figs. 1 and 2 and for the M(3000)F2 models in Figs. 5 and 6. From Fig. 1 it can be seen that for the vast majority of the stations considered, an accuracy higher than 5% is achieved in 20–40% of the cases, an accuracy higher than 10% in 40–60%, an accuracy higher than 15% in 60–80%. Moreover, it has been shown that *foE* plays an important role in the performance of this model since in the northernmost stations (e.g. Lycksselle) the accuracy is degraded in winter where the daytime duration is very short and hence *foE* cannot affect the model adequately. A closer look at Fig. 1 reveals a symmetry with characteristic accuracy degradation in the equinoxes and an increase in summer. This could be related to an enhancement in the *fo*F2 variability during the spring and autumn months.

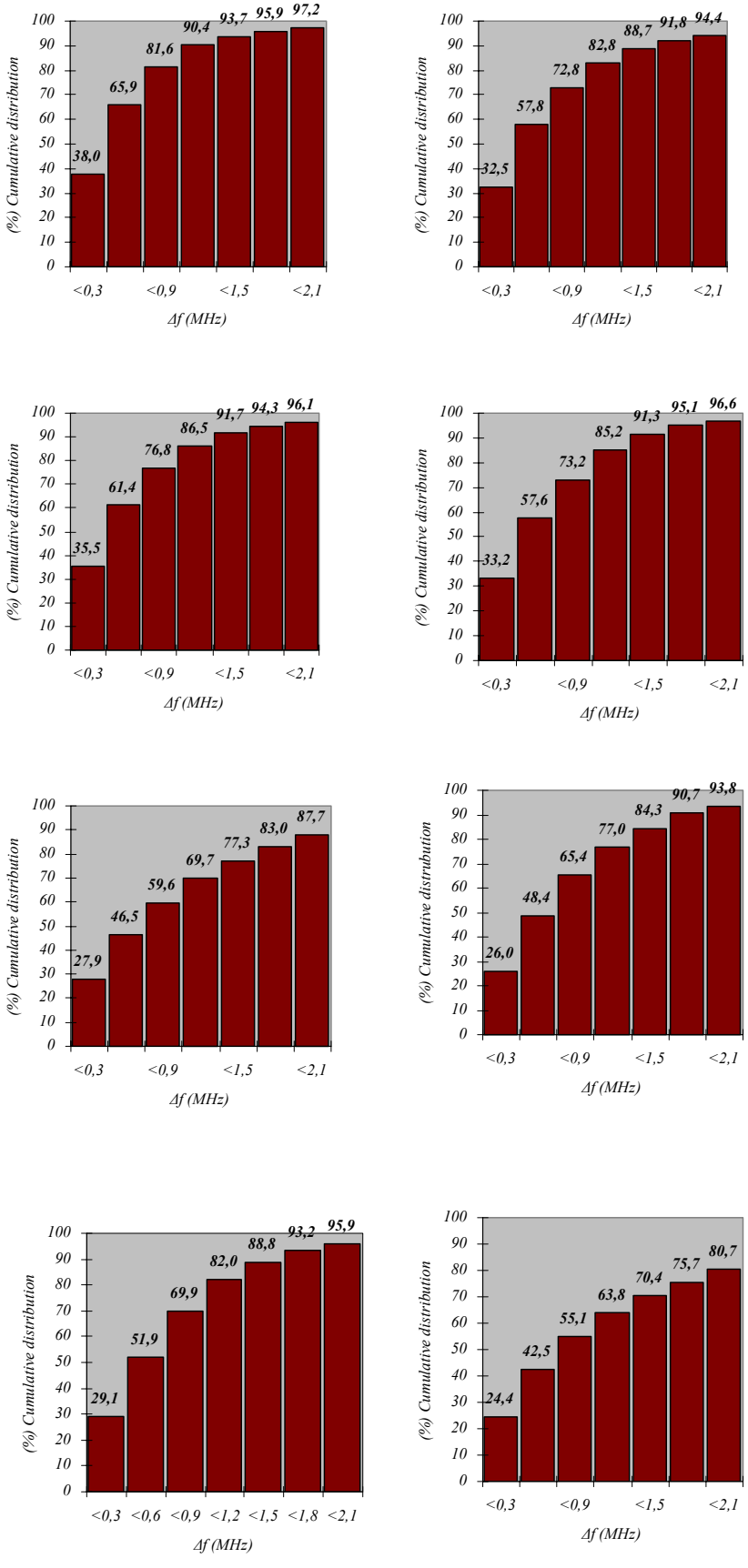

Fig. 3. Performance of *fo*F2 single station model for Kiev and for January, March, June and November.

Fig. 4. Performance of *fo*F2 mapping model for Kiev and for January, March, June and November.

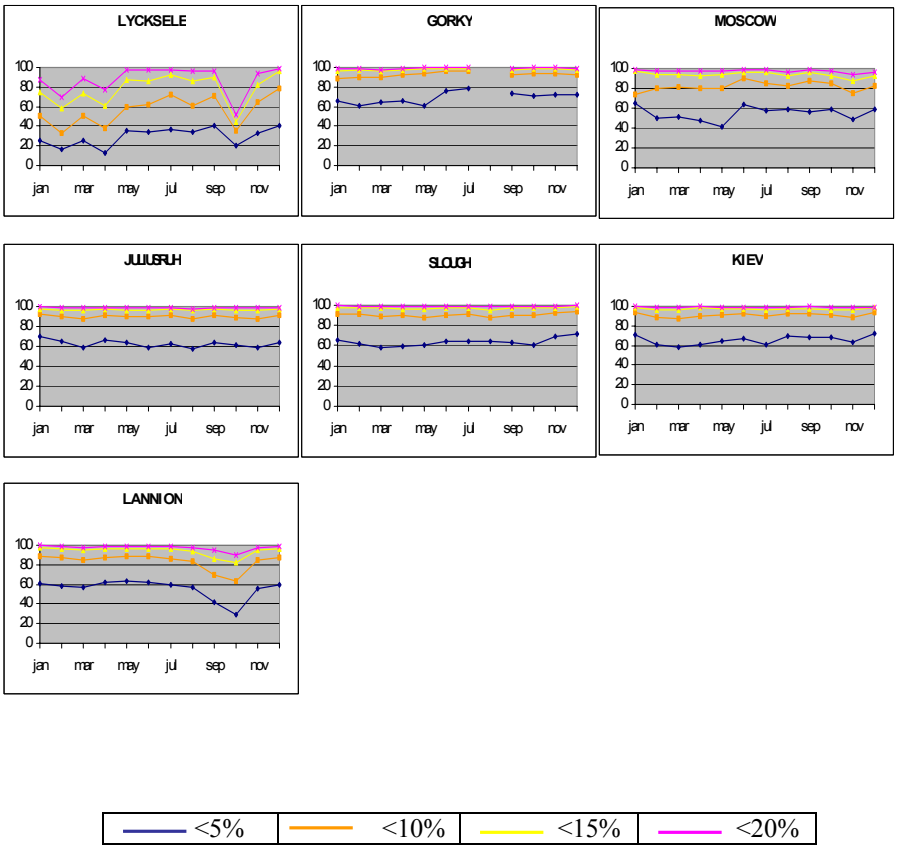

Fig. 5. Performance of the M(3000)F2 single station model for each ionospheric station.

Table 3. Model inputs

*fo*F2 SSM	*fo*F2 Mapping	M(3000)F2 SSM	M(3000)F2 Mapping
foE_{12}	FoE_{12}	foE_{12}	foE_{12}
$foF2_{12\,odb}$ one day before	$foF2_{12\,odb}$ one day before at Juliusruh	$f'oE$	$foF2_{12\,odb}$ one day before at Juliusruh
		$\cos\chi_{12}$	

(Kouris et al., 1998, 1999).

The results of the second model for F2, which is characterized as an electronic mapping model, are summarized in Fig. 2. From this figure, it can be seen that for the vast majority of the stations considered, an accuracy higher than 5% is achieved in 10–20% of the cases, an accuracy higher than 10% in 10–40%, an accuracy higher than 15% in 10–60% of the cases whereas a better accuracy than 20% can be reached in 10–80% of the cases. The symmetry observed in the former model is also seen in this one but the main difference is that there is a strong degradation in accuracy during January and December. Comparing the accuracies achieved by these two models, it can be deduced that although model 2 performs very well in most of the cases, it is generally less accurate. Of course, it has to be stressed that this model is rather an electronic mapping model than a single station model, and consequently such a degradation performance is to be expected. In this model, the geographic latitude influence is also evident, since stations on almost the same geographical latitude as Juliusruh is, which is the reference point for this model, present much higher accuracy than the southernmost or northernmost stations, especially during wintertime. Figures 3 and 4 present the performance of both *fo*F2 models (single station and mapping) at Kiev and for January, March, June and November. It can be seen that well above 60% of the predictions are with an error of less than 0.6 MHz.

The performance of the M(3000)F2 single station models are presented in Fig. 5. From this figure, it can be observed that for the vast majority of the stations considered, an accuracy higher than 5% is achieved in 60–80% of the cases, an accuracy higher than 10% in 80–90%, an accuracy higher than 15% in 90%. This could be due to the fact that the variability of M(3000)F2 is much lower than that of *fo*F2. (Kouris et al., 1998, 1999) The performance of the M(3000)F2 mapping models are presented in Fig. 6. From this figure it can be seen that for the equilatitudinal stations

Table 4. Prediction reliability investigation for selected ionospheric stations for the *fo*F2 single station model for various solar and geomagnetic conditions

Station	Accuracy	$A_p \leq 40$	$A_p > 40$	$R \leq 60$	$60 < R \leq 110$	$R > 110$
Dourbes	5%	33,03%	29,50%	34,06%	32,31%	28,11%
	5–10%	24,53%	24,83%	24,34%	26,06%	23,66%
	10–15%	16,71%	20,00%	16,47%	17,68%	17,30%
	15–20%	10,78%	10,16%	10,81%	10,62%	10,72%
Ebre	5%	32,49%	32,17%	32,30%	33,96%	31,32%
	5–10%	24,48%	24,29%	24,53%	24,38%	24,38%
	10–15%	16,68%	16,08%	16,53%	16,56%	17,01%
	15–20%	10,47%	9,74%	10,80%	9,80%	10,12%
Kalliningrad	5%	29,66%	30,40%	26,57%	30,72%	34,34%
	5–10%	23,32%	23,06%	22,01%	23,76%	25,19%
	10–15%	17,09%	17,11%	17,47%	17,30%	16,27%
	15–20%	11,11%	10,61%	12,03%	10,76%	9,67%
Miedzeszyn	5%	37,94%	35,41%	37,76%	42,29%	No data
	5–10%	26,48%	21,25%	26,42%	19,16%	No data
	10–15%	15,39%	14,27%	15,34%	15,62%	No data
	15–20%	8,59%	12,50%	8,72%	9,79%	No data
Slough	5%	29,47%	29,45%	25,80%	32,28%	33,34%
	5–10%	23,80%	23,16%	22,61%	24,79%	24,88%
	10–15%	16,68%	16,91%	17,21%	16,28%	16,16%
	15–20%	11,12%	10,41%	12,22%	10,21%	9,87%
Uppsala	5%	20,21%	20,76%	17,82%	20,03%	20,58%
	5–10%	18,19%	17,80%	18,77%	18,69%	18,04%
	10–15%	15,18%	16,39%	16,63%	15,65%	15,00%
	15–20%	11,52%	11,52%	11,75%	11,97%	11,31%

Table 5. Prediction reliability investigation for selected ionospheric stations, for the *fo*F2 mapping and for various solar and geomagnetic conditions

Station	Accuracy	$A_p \leq 40$	$A_p > 40$	$R \leq 60$	$60 < R \leq 110$	$R > 110$
Dourbes	5%	22,69%	20,16%	22,99%	24,86%	18,11%
	5–10%	20,58%	16,66%	20,83%	22,32%	16,52%
	10–15%	17,19%	19,66%	17,01%	18,04%	17,44%
	15–20%	12,86%	12,83%	12,89%	12,90%	12,61%
Ebre	5%	21,79%	18,57%	24,86%	23,55%	17,01%
	5–10%	19,52%	16,86%	20,83%	21,53%	16,32%
	10–15%	16,49%	20,68%	18,01%	19,43%	18,65%
	15–20%	13,56%	13,83%	12,57%	11,99%	11,32%
Juliusruh Reference station						
Miedzeszyn	5%	24,23%	13,28%	23,31%	18,75%	No data
	5–10%	23,81%	15,23%	22,85%	23,95%	No data
	10–15%	18,03%	14,97%	17,62%	19,27%	No data
	15–20%	12,30%	12,50%	12,23%	13,80%	No data
Slough	5%	21,98%	23,80%	19,25%	23,66%	24,50%
	5–10%	19,71%	20,93%	18,32%	20,67%	20,98%
	10–15%	16,34%	16,78%	16,88%	15,91%	16,02%
	15–20%	12,61%	11,58%	14,48%	11,83%	10,65%
Uppsala	5%	12,77%	14,04%	17,12%	13,10%	12,41%
	5–10%	11,90%	13,81%	16,61%	12,06%	11,67%
	10–15%	10,46%	12,61%	14,27%	10,55%	10,32%
	15–20%	8,49%	8,53%	9,09%	8,82%	8,29%

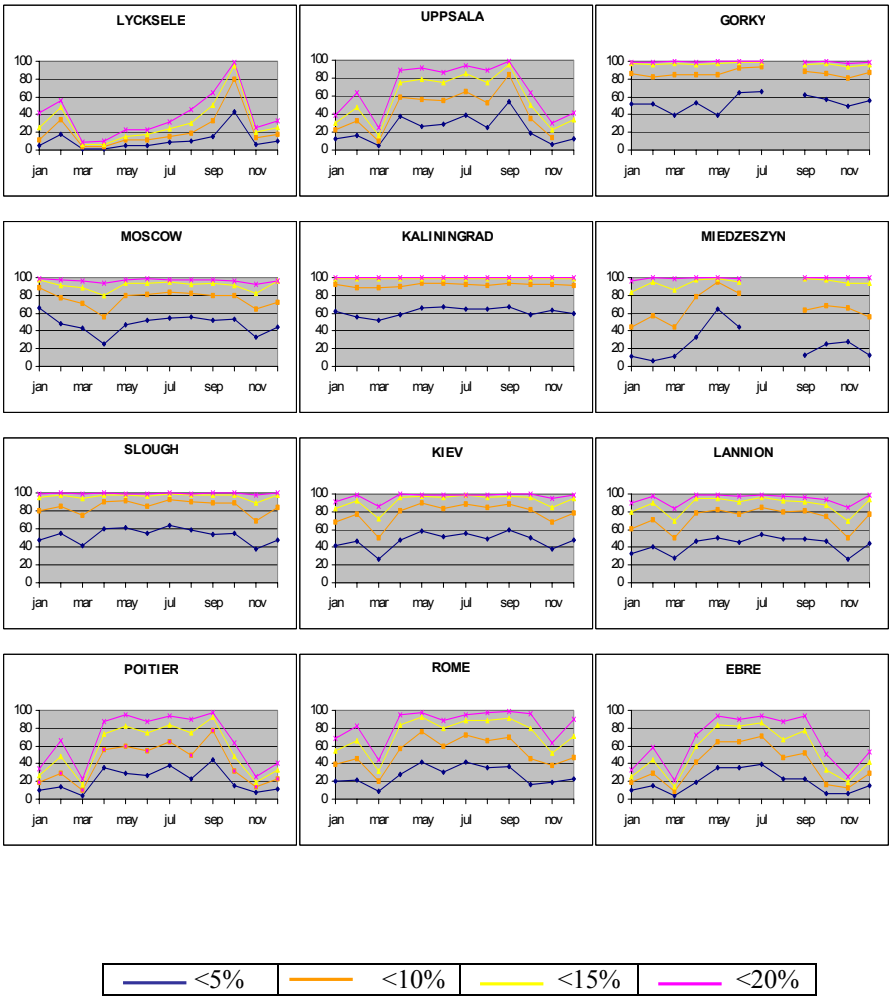

Fig. 6. Performance of M(3000)F2 electronic mapping technique for each ionospheric station.

considered, accuracy higher than 5% is achieved in 20–60% of the cases, accuracy higher than 10% in 60–80%, accuracy higher than 15% in 80–90%. Yet for the northernmost and southernmost station the above accuracies were degraded to 10–60%, 20–80% and 20–90%, respectively.

To further investigate the performance of the above four models in various ionospheric conditions, the errors obtained were categorized with respect to solar and geomagnetic conditions taking into account the R and A_p indices. Then the solar activity was divided in three categories (Bradley et al., 1995) namely $R < 60$ (low solar activity), $60 < R < 140$ (medium solar activity) and $R > 110$ (high solar activity) and A_p into two; $A_p < 40$ (quite ionosphere) and $A_p > 40$ (disturbed ionosphere). Selected results for the *fo*F2 models only are presented in Tables 4 and 5. M(3000)F2 models are not further investigated since their accuracy is very high and they do not seem to be affected by the above parameters. From Tables 4 and 5, it can be deduced that the accuracy of the *fo*F2 models is hardly affected by the solar activity although the geomagnetic activity affects them to some extent, degrading the prediction accuracy.

In order to examine the performance of the single station and mapping models under strong geomagnetic and solar activity conditions, *fo*F2 data from three selected ionospheric stations were chosen (Tables 6 and 7). The criterion for choosing these stations was that that they were northern stations and therefore they were liable to suffer strongly under the above stressful conditions. M(3000)F2 was not considered again since its variability is low and the prediction accuracy is always very high. From Table 6 it can be seen that there is no clear evidence that simultaneous increase of A_p and R can degrade the accuracy of the single station models; on the contrary, there is evidence that their accuracy increases at medium solar activity independently of the geomagnetic activity. The same are to be seen in Table 7 when the mapping model is considered. Yet, as it can be seen from all tables referring to *fo*F2, the local variability (Kouris, 2002a, 2002b) can play an important role to the performance of the models since the larger categories of errors ($> 20\%$) remain stable regardless of geomagnetic or solar conditions.

Table 6. *fo*F2 Single station models performance for selected ionospheric stations under stressful solar and geomagnetic conditions

Station	Accuracy	$R \leq 60$		$60 < R \leq 110$		$R > 110$	
		$A_p \leq 80$	$A_p > 80$	$A_p \leq 80$	$A_p > 80$	$A_p \leq 80$	$A_p > 80$
Dourbes	$> 5\%$	34.08	30.83	32.33	29.16	28.24	8.33
	$> 10\%$	58.45	50.83	58.37	58.32	51.84	41.63
	$> 15\%$	74.91	69.16	76.01	83.32	69.09	66.63
Slough	$> 5\%$	25.81	25.00	32.31	30.20	33.33	33.50
	$> 10\%$	48.43	47.08	57.11	54.15	58.25	56.59
	$> 15\%$	65.56	63.33	73.43	67.17	74.38	74.12
Uppsala	$> 5\%$	18.22	16.66	20.11	12.50	20.44	25.00
	$> 10\%$	35.25	33.32	38.75	35.41	38.42	44.12
	$> 15\%$	52.27	52.07	54.39	53.11	53.30	63.05

Table 7. *fo*F2 Mapping technique performance for selected ionospheric stations under stressful solar and geomagnetic conditions

Station	Accuracy	$R \leq 60$		$60 < R \leq 110$		$R > 110$	
		$A_p \leq 80$	$A_p > 80$	$A_p \leq 80$	$A_p > 80$	$A_p \leq 80$	$A_p > 80$
Dourbes	$> 5\%$	23.04	15.00	24.74	45.83	18.12	16.66
	$> 10\%$	43.95	23.33	47.05	70.83	34.61	37.49
	$> 15\%$	60.99	36.66	65.06	95.83	52.07	37.49
Slough	$> 5\%$	12.27	16.66	23.64	25.52	24.49	25.17
	$> 10\%$	37.61	32.40	44.31	46.35	45.42	48.26
	$> 15\%$	54.48	51.84	60.21	63.01	61.45	63.88
Uppsala	$> 5\%$	17.13	16.66	12.99	23.95	12.36	15.34
	$> 10\%$	33.64	37.59	24.96	44.82	26.93	31.05
	$> 15\%$	47.85	54.15	35.51	56.23	34.25	41.27

4 Conclusions

In this paper Neural-Network-based single-station hourly daily *fo*F2 and M(3000)F2 modelling of 15 European ionospheric stations has been investigated. Two types of models were presented for the F2-layer critical frequency prediction and two for the propagation factor M(3000)F2. The first type of models was a single station model whereas the second type introduced a new regional mapping technique, employing Juliusruh neural network relevant models. The predicted values were compared to the corresponding measured data, the relative errors were calculated and the predicted periods were categorised according to the geomagnetic (with respect to A_p) and solar (with respect to R) conditions into quiet and disturbed ionosphere, and low, medium and high solar activity. Depending on the type of data and on the month, the resulting correlation seems to vary from good to very good and what is more important, the results do not seem to be affected considerably by geomagnetic or solar conditions. Moreover, it is worth mentioning that the new mapping technique gives very promising results.

References

Alberca, L. F., Juchnikowski, G., Kouris, S. S., Mikhailov, A. V., Mikhailov, V. V., Miro, G., delaMorena, B., Mukhtarov, P., Panceva, D., Sole, G. J., Stanislawska, I., Villanueva, L., and Xenos, Th.: Comparison of various single station models for European area, Acta Geoph. Polonica, XLVII. 1, 77–91.

Altynay, O., Tulunay, E., and Tulunay, Y.: Forecasting of Ionospheric critical frequency using neural networks, Geophys. Res. Lett., 1467–1440, 1996.

Bradley, P. A., Kouris, S. S., Xenos, Th., and Dick, M. I.: Reference *fo*F2 measurement data set for long-term temperate-latitude regional mapping, Adv. Space Res., 16.1, 163–166.

Cander, L. R., Milosavljevic, M. M., Stankovicz, S. S., and Tomasevic, S.: Ionospheric forecasting technique by artificial neural network, Electronic Letters, 34.16, 1573–1574, 1998.

Kouris, S. S.: Solar and latitude dependence of E-region critical frequence, Il Nuovo Cimento, 4C. 4, 417–430, 1981.

Kouris, S. S. and Nissopoulos, J. K.: Variation of *fo*F2 with solar activity, Adv. in Space Res., 14.12, 51–54, 1994.

Kouris, S. S., Fotiadis, D. N., and Xenos, T. D.: On the day to day variation of *fo*F2 and M(3000)F2, Adv. Space Res., 22.6, 873–876, 1998.

Kouris, S. S., Fotiadis, D. N., and Zolesi, B.: Specifications of the F-region variations for quiet and disturbed conditions, Phys. Chem.

Earth, 24.4, 321–327, 1999.
Kouris, S. S. and Fotiadis, D. N.: Ionospheric variability: A comparative statistical study, Adv. Space Res., 29.6, 977–985, 2002a.
Kouris, S. S. and Fotiadis, D. N.: A quantitative description of the ionospheric varability – Preliminar results, Acta Geod. Geoph. Hung., 37.2–3, 309–312, 2002b.
Kumulca, A., Tulunay, E., Topalli, I., and Tulunay, Y.: Temporal and spatial forecasting of ionopsheric critical frequency using neural networks, Radio Sci, 34.6, 1497–1506, 1999.
Pancheva, D. and Mukhtarov Pl.: A single-station spectral model of the monthly median F-region critical frequency, Annali di Geof., 39.4, 807–818, 1996.
Sole, J. G.: Relations between hourly monthly median values of *fo*F2 and some geophysical indices. Their application to an ionospheric single station model, Acta Geophys. Polonica, XLVI, 77–88, 1998.
Williscroft, L. A. and Poole, A. W. V.: Neural networks, *fo*F2, sunspot number and magnetic activity, Geophys. Res. Lett., 23.24, 3659–3662, 1996.
Xenos, Th.: A single station model suitable for *fo*F2 mapping, Annali di Geofisica, 42.1, 129–135, 1999.